

Measurement of tau Michel parameters

Nobuhiro Shimizu for the Belle collaboration^{*†}

University of Tokyo, Aihara/Yokoyama laboratory,

Department of Physics, 7-3-1 Hongo, Bunkyo-ku, Tokyo 113-0033 JAPAN

E-mail: shimizu@hep.phys.s.u-tokyo.ac.jp[‡]

The Michel parameters are fundamental characteristics of μ and τ leptons which determine the kinematic distribution of daughter particles from their leptonic decays. The comparison of experimentally-measured values versus the Standard model predictions allows us to test the Lorentz structure of weak interaction in model independent way. We review the tau Michel parameter measurements performed before and present our recent measurements by Belle experiments.

Flavor Physics and CP Violation

5-9 June 2017

Hotel Don Giovanni, Prague, Czech Republic

^{*}Speaker.

[†]Belle collaboration.

[‡]Present address is shimizu@champ.hep.sci.osaka-u.ac.jp

1. Introduction

The decay of tau is known as one of the most important tools to search for New Physics (NP). The large mass of τ ($m_\tau = 1776.86 \pm 0.12$ MeV [1]) allows us to expect an enhancement of the sensitivity to the NP. For instance, the NP models such as 2HDM (two Higgs doublet model) predict the existence of charged Higgs and the magnitude of their couplings are proportional to mass of leptons. Therefore, in comparison with muon decays, we can expect the gain of a factor $(m_\tau/m_\mu)^2 \sim 300$ in the simplest case.

The mass of τ makes it possible to decay into both leptons and hadrons. The former one is called *leptonic* decay and accounts for approximately 35% of all tau decays. Various properties of these decays, described by the electroweak sector of the SM, are precisely calculated, hence experimental results can be definitely compared with theoretical predictions. The rest decays of tau contain hadrons in the final state and called *hadronic* decay. These decays turn out to be beautiful laboratory for studying low energy structure of the strong interaction like the chiral perturbation theory.

Both of these decay are mediated by the weak interaction. In the Standard Model (SM), the Lorentz structure of corresponding intermediate particle, W^\pm boson, includes the vector and axial-vector contributions in the same magnitude with opposite sign and turns out to maximally violate the symmetry of parity (so called $V - A$ structure). Thus the precision test of this structure may reveal hints from the Physics Beyond the Standard Model (BSM) and the measurement of Michel parameters of tau lepton offers an ideal laboratory to us.

2. Michel Parameters

The most general Lorentz-invariant derivative-free matrix element of leptonic τ decay $\tau^- \rightarrow \ell^- \nu \bar{\nu}^*$ is represented as [2, 3]

$$\mathcal{M} = \begin{array}{c} \begin{array}{ccc} & \nu_\tau & \\ & \nearrow & \\ \tau & \bullet & \text{---} W \text{---} \bullet \\ & \searrow & \\ & \nu_\ell & \end{array} \\ \begin{array}{ccc} & \nu_\ell & \\ & \nearrow & \\ \ell & \bullet & \end{array} \end{array} = \frac{4G_F}{\sqrt{2}} \sum_{\substack{N=S,V,T \\ i,j=L,R}} g_{ij}^N [\bar{u}_i(\ell)\Gamma^N v_n(\nu_\ell)] [\bar{u}_m(\nu_\tau)\Gamma_N u_j(\tau)],$$

where G_F is the Fermi constant, i and j are the chirality indices for the charged leptons, n and m are the chirality indices of the neutrinos, ℓ is e or μ , $\Gamma^S = 1$, $\Gamma^V = \gamma^\mu$ and $\Gamma^T = i(\gamma^\mu \gamma^\nu - \gamma^\nu \gamma^\mu)/2\sqrt{2}$ are, respectively, the scalar, vector and tensor Lorentz structures in terms of the Dirac matrices γ^μ , u_i and v_i are the four-component spinors of a particle and an antiparticle, respectively, and g_{ij}^N are the corresponding dimensionless couplings. In the SM, τ^- decays into ν_τ and W^- boson, the latter decays into ℓ^- and right-handed $\bar{\nu}_\ell$, *i.e.*, the only non-zero coupling is $g_{LL}^V = 1$. Experimentally, only the squared matrix element is observable and bilinear combinations of the g_{ij}^N are accessible. Of all such combinations, four Michel parameters, η , ρ , δ and ξ , can be measured in the leptonic decay of the τ when the final-state neutrinos are not observed or the spin of the outgoing lepton is

*Unless otherwise stated, use of charge-conjugate modes is implied throughout the paper.

not measured [4]:

$$\rho = \frac{3}{4} - \frac{3}{4} \left(|g_{LR}^V|^2 + |g_{RL}^V|^2 + 2|g_{LR}^T|^2 + 2|g_{RL}^T|^2 + \Re(g_{LR}^S g_{LR}^{T*} + g_{RL}^S g_{RL}^{T*}) \right), \quad (2.1)$$

$$\eta = \frac{1}{2} \Re(6g_{RL}^V g_{LR}^{T*} + 6g_{LR}^V g_{RL}^{T*} + g_{RR}^S g_{LL}^{V*} + g_{RL}^S g_{LR}^{V*} + g_{LR}^S g_{RL}^{V*} + g_{LL}^S g_{RR}^{V*}), \quad (2.2)$$

$$\xi = 4\Re(g_{LR}^S g_{LR}^{T*} - g_{RL}^S g_{RL}^{T*}) + |g_{LL}^V|^2 + 3|g_{LR}^V|^2 - 3|g_{RL}^V|^2 - |g_{RR}^V|^2 + 5|g_{LR}^T|^2 - 5|g_{RL}^T|^2 + \frac{1}{4} \left(|g_{LL}^S|^2 - |g_{LR}^S|^2 + |g_{RL}^S|^2 - |g_{RR}^S|^2 \right), \quad (2.3)$$

$$\xi \delta = \frac{3}{16} \left(|g_{LL}^S|^2 - |g_{LR}^S|^2 + |g_{RL}^S|^2 - |g_{RR}^S|^2 \right) - \frac{3}{4} \left(|g_{LR}^T|^2 - |g_{RL}^T|^2 - |g_{LL}^V|^2 + |g_{RR}^V|^2 - \Re(g_{LR}^S g_{LR}^{T*} + g_{RL}^S g_{RL}^{T*}) \right). \quad (2.4)$$

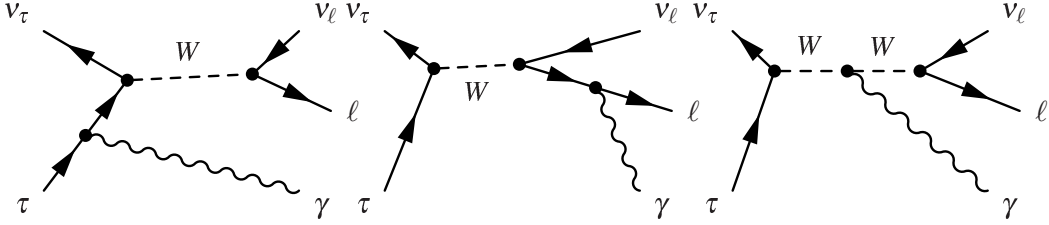


Figure 1: Three Feynman diagrams of the tau radiative leptonic decay

The Feynman diagrams describing the radiative leptonic decay of the τ are presented in Fig. 1. The last amplitude is ignored because this contribution turned out to be suppressed by the very small factor $(m_\tau/m_W)^2$ [5]. As shown in Refs. [6, 7], through the presence of a radiative photon in the final state, the polarization of the outgoing lepton is indirectly exposed, accordingly two more Michel parameters $\bar{\eta}$ and $\xi \kappa$ become experimentally accessible:

$$\bar{\eta} = |g_{RL}^V|^2 + |g_{LR}^V|^2 + \frac{1}{8} \left(|g_{RL}^S + 2g_{RL}^T|^2 + |g_{LR}^S + 2g_{LR}^T|^2 \right) + 2 \left(|g_{RL}^T|^2 + |g_{LR}^T|^2 \right), \quad (2.5)$$

$$\xi \kappa = |g_{RL}^V|^2 - |g_{LR}^V|^2 + \frac{1}{8} \left(|g_{RL}^S + 2g_{RL}^T|^2 - |g_{LR}^S + 2g_{LR}^T|^2 \right) + 2 \left(|g_{RL}^T|^2 - |g_{LR}^T|^2 \right). \quad (2.6)$$

- η and ρ

Two η and ρ are spin-independent Michel parameters, *i.e.*, their effects are irrelevant to the polarization of tau lepton. Figure 2 shows an energy distribution of muon in $\tau^- \rightarrow \mu^- \nu \bar{\nu}$ decay for various η and ρ values. ρ parameter mainly affects the high energy part in the spectrum while η is not; thus η is sometimes called *low-energy* parameter.

Important characteristics of η is that it is the *first order* in terms of New Physics, unlike other Michel parameters. According to Eq. (2.2) and noting $g_{LL}^V \sim 1$, $\eta \sim 0.5\Re\{g_{RR}^S\}$. Indeed, η

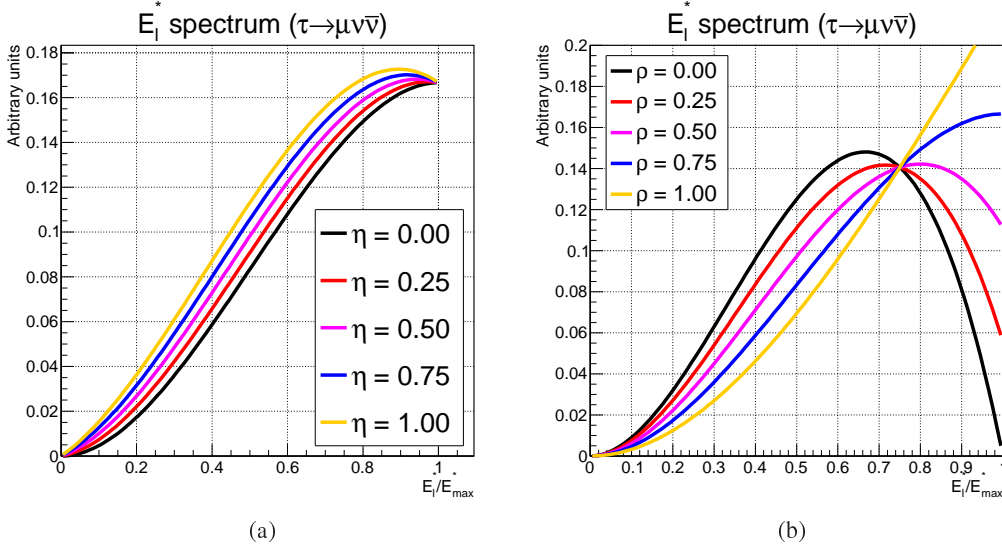


Figure 2: Dependence of the energy of daughter muon in the tau rest frame on (a) η and (b) ρ ($\tau^- \rightarrow \mu^- \nu \bar{\nu}$ decay). Horizontal axis is normalized in terms of maximum energy $E_{\max} = (m_\tau^2 + m_\ell^2)/2m_\tau$.

parameter is related to New Physics variables of the 2HDM [8]:

$$\eta = -\frac{m_\tau m_\ell}{2} \left(\frac{\tan \beta}{m_{H^\pm}} \right)^2, \quad (2.7)$$

where m_τ , m_ℓ and m_{H^\pm} are masses of tau, daughter lepton and charged Higgs, respectively, β is a ratio of vacuum expectation value between up-type and down-type quarks. Unfortunately, the effects from η is suppressed by the small mass of daughter lepton. More explicitly, the generalized branching ratio can be written by

$$\frac{\mathcal{B}(\tau^- \rightarrow \ell^- \nu \bar{\nu})}{\mathcal{B}_{SM}(\tau^- \rightarrow \ell^- \nu \bar{\nu})} = 1 + \eta \frac{m_\ell}{m_\tau}, \quad (2.8)$$

thus it is difficult to measure η parameter from the electron mode $\tau^- \rightarrow e^- \nu \bar{\nu}$.

ρ parameter is used to constrain magnitude of each coupling coefficient. $1 - \rho$ can be written by

$$1 - \rho = \frac{1}{16} |g_{LL}^S|^2 + \frac{1}{16} |g_{RR}^S|^2 + \frac{1}{4} |g_{LL}^V|^2 + \frac{1}{4} |g_{RR}^V|^2 + |g_{LR}^V|^2 + |g_{RL}^V|^2 + \frac{1}{16} |g_{LR}^S + 6g_{LR}^T|^2 + \frac{1}{16} |g_{RL}^S + 6g_{RL}^T|^2 \quad (2.9)$$

and the right hand side of Eq. (2.9) is non-negative. It is thus, the experimental value can give upper limit.

- ξ and $\xi \delta$

Unlike above η and ρ parameters, ξ and $\xi \delta$ are *spin-dependent* parameters. These two

parameters are included in the differential decay width together with the spin vector of tau lepton. The measurement requires, therefore, the extraction of tau-spin information. Experimentally, the spin-spin correlation of tau leptons in the annihilation process $e^+e^- \rightarrow \tau^+\tau^-$ is utilized [9]. Polarization of both taus are anti-correlated each other and consequently an observation of spectra of decay products from both taus makes it possible to extract ξ and $\xi\delta$ parameters.

Of particular interest of these two parameters is the fact that the normalized probability that right-handed tau lepton couples with W^- boson, Q_{τ_R} , can be calculated by combining ξ and $\xi\delta$ parameters:

$$Q_{\tau_R} = \frac{1}{2} \left(1 + \frac{1}{3}\xi - \frac{16}{9}\xi\delta \right). \quad (2.10)$$

This is forbidden in the SM and the experimental value of $Q_{\tau_R} = 0.00 \pm 0.02^\dagger$ is consistent with the SM prediction.

- $\bar{\eta}$ and $\xi\kappa$

$\bar{\eta}$ and $\xi\kappa$ are additional parameters which can be measured only through the observation of the radiative leptonic decays $\tau^- \rightarrow \ell^- \nu \bar{\nu} \gamma$. The angular distribution of photon versus the spectrum of daughter lepton exposes the polarization of daughter lepton and this is reflected on the appearance of new parameters.

$\bar{\eta}$ appears in spin-independent terms of the differential decay width of $\tau^- \rightarrow \ell^- \nu \bar{\nu} \gamma$. Since all terms in Eq. (2.5) are strictly non-negative, similarly to $1 - \rho$ situation, the upper limit on $\bar{\eta}$ provides a constraint on each coupling constant as well.

On the other hand, $\xi\kappa$ is a spin-dependent parameter and this measurement requires the tau spin information. According to Ref. [10], $\xi\kappa$ is related to the normalized probability that the τ^- decays into the right-handed charged daughter lepton $Q_{\ell_R} = (1 + \xi + 4\xi\kappa - 8\xi\delta/3)/2$ [11].

In muon decay, through the direct measurement of electron polarization in $\mu^+ \rightarrow e^+ \nu \bar{\nu}$, equivalent parameters ξ' and $\xi'' = 16\rho/3 - 4\bar{\eta} - 3$ (see Table 1) have been already measured, whereas $\bar{\eta}$ and $\xi\kappa$ of the τ lepton have not been measured yet. Therefore, the measurement of both parameters provides a further constraint on the Lorentz structure of the weak current.

- Summary of six parameters

Table 1 summarizes the information of described Michel parameters. In addition to the explained parameters, we also included η'' , ξ' and ξ'' . Figure 3 shows illustrative summary of various parameters by several experiments. The combined averages by Particle Data Group (PDG) are consistent with the SM prediction within their uncertainties, where these uncertainties vary 1% to 3%. All of these measurements were carried out approximately twenty years ago and the update is desired using modern B factories.

[†] Calculated based on the PDG value

Table 1: Michel parameters of the τ lepton [†]

Name	SM value	Spin correlation	Experimental result [1]	Comments and Ref.
η	0	no	0.013 ± 0.020	(ALEPH) [12]
ρ	3/4	no	0.745 ± 0.008	(CLEO) [13]
$\xi\delta$	3/4	yes	0.746 ± 0.021	(CLEO) [13]
ξ	1	yes	1.007 ± 0.040	measured in leptonic decays (CLEO) [13]
ξ_h	1	yes	0.995 ± 0.007	measured in hadronic decays (CLEO) [13]
$\bar{\eta}$	0	no	not measured	from radiative decay (RD)
$\xi\kappa$	0	yes	not measured	from RD
η''	0	no	not measured	from RD, suppressed by m_l^2/m_τ^2
ξ'	1	yes	-	$\xi' = -\xi - 4\xi\kappa + 8\xi\delta/3$.
ξ''	1	no	-	$\xi'' = 16\rho/3 - 4\bar{\eta} - 3$.

[†] Experimental results represent average values obtained by PDG [1].

3. Measurements of Michel parameters by Belle experiments

Utilizing the large number of statistics of tau lepton by B factory as well as the precise description of probability density function, Belle collaboration measures η , ρ , ξ and $\xi\delta$ parameters from $\tau^- \rightarrow \ell^- \nu \bar{\nu}$ decay to achieve precision better than 1%. Whereas from the radiative decay $\tau^- \rightarrow \ell^- \nu \bar{\nu} \gamma$, the $\bar{\eta}$ and $\xi\kappa$ are measured. The latter represents the first measurement of these parameters for the tau lepton. Both of two analyses use $\tau \rightarrow \rho(\rightarrow \pi\pi^0)\nu$ decay in the partner side of tau and the spin-spin correlation of $\tau\tau$ pair to extract the information of signal τ lepton.

3.1 Belle experiment

The Belle experiment at KEK (Tsukuba, Japan) collected 1040 fb^{-1} of data sample using e^+e^- energy-asymmetric collider KEKB and Belle detector. It ran from June 1999 to June 2010 and contributed to the progress of high energy physics. The Belle detector is designed to be multi-purpose so that vertexing, momentum tracking, energy measurement of photon and particle identification are interactively performed by several sub-detectors.

These B factory experiments are useful laboratory also for the study of the τ leptons. At the resonance energy of $\Upsilon(4S) \sim 10.58 \text{ GeV}$, the cross section of tau pair production is compatible with that of bb pair ($\sigma_{ee \rightarrow \tau\tau} = 0.9 \text{ nb}^{-1}$ and $\sigma_{ee \rightarrow bb} = 1.1 \text{ nb}^{-1}$). Indeed, spending approximately ten years, KEKB accelerator and Belle detector collected $O(10^9)$ of $\tau\tau$ pair data.

3.2 τ spin extraction

To measure ξ , $\xi\delta$, $\xi\kappa$ parameters, the spin of τ must be measured. This is extracted using the spin-spin correlation of tau lepton pairs. In the beam energy of KEKB accelerator, the chirality of tau leptons are anti-correlated by $\sim 95\%$, thus once we measure the spin of the other side of tau lepton, or tag side, we can extract the spin of signal tau lepton. In the tag side, we use $\tau \rightarrow \rho\nu \rightarrow$

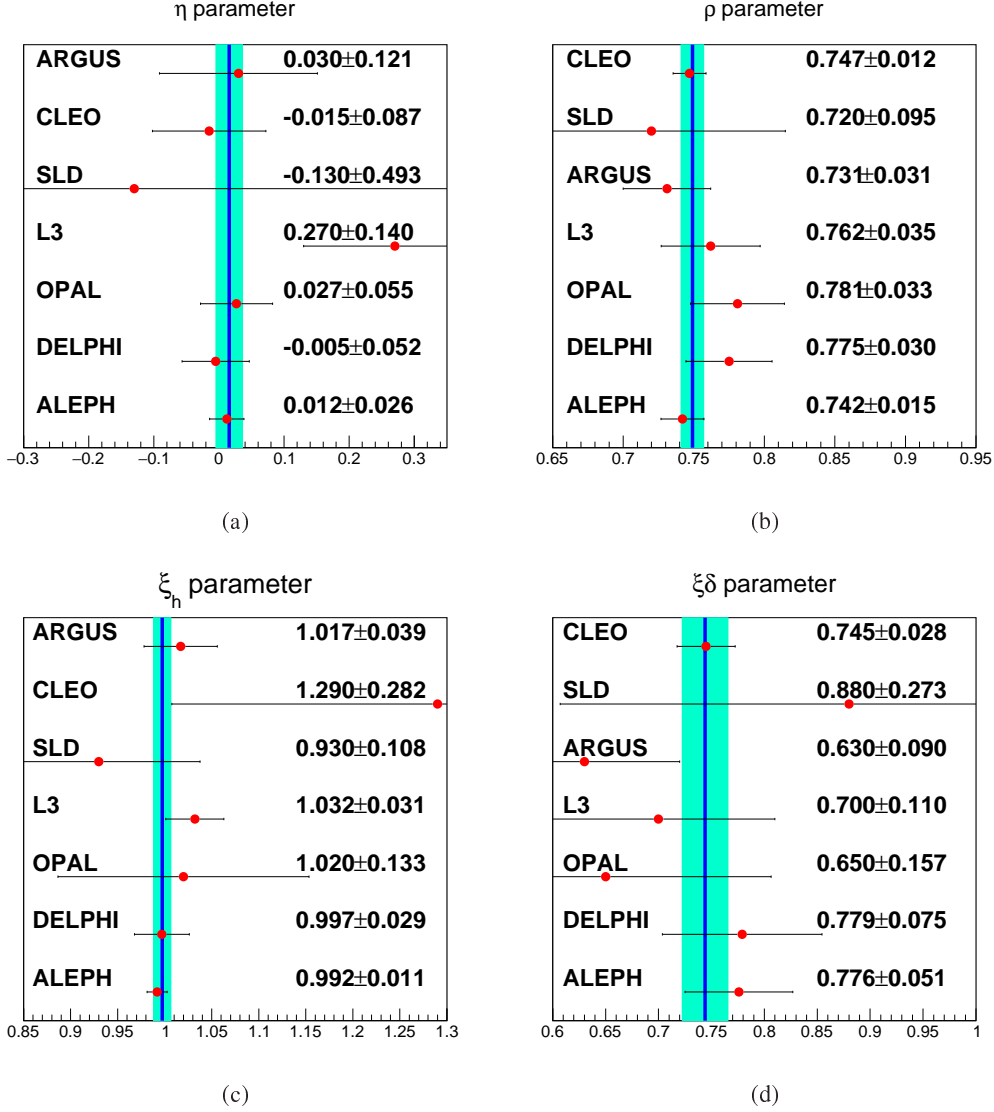


Figure 3: Summary of the measured Michel parameters: (a) η (b) ρ (c) ξ_h and (d) $\xi\delta$. Lines and filled regions are the combined values and their uncertainties summarized in Table 1.

$\pi\pi^0\nu$ decay mode as a *spin-analyzer*. Indeed, the differential decay width of $\tau \rightarrow \rho\nu \rightarrow \pi\pi^0\nu$ is written by

$$d\Gamma(\tau \rightarrow \rho\nu \rightarrow \pi\pi^0\nu) \propto A + \vec{B} \cdot \vec{S}_\tau, \quad (3.1)$$

where A and \vec{B} are known functions of kinematic variables of π and π^0 , and \vec{S}_τ is a spin of τ . Equation (3.1) represents there is a sensitivity to the spin. For more details, see Refs. [15, 16].

3.3 Extraction of Michel parameters

Combining the kinematic observables of both signal and tag sides, the phase space of an event forms multi-dimension variables: $\vec{x} = \{P_\ell, \Omega_\ell, P_\rho, \Omega_\rho, m_{\pi\pi}^2, \tilde{\Omega}_\pi\}$ for η , ρ , ξ and $\xi\delta$ measurement

using $\tau^- \tau^+ \rightarrow (\ell^- \nu \bar{\nu})(\rho^+ \bar{\nu})$ and $\vec{x} = \{P_\ell, \Omega_\ell, P_\gamma, \Omega_\gamma, P_\rho, \Omega_\rho, m_{\pi\pi}^2, \tilde{\Omega}_\pi\}$ for $\bar{\eta}$ and $\xi \kappa$ measurement using $\tau^- \tau^+ \rightarrow (\ell^- \nu \bar{\nu} \gamma)(\rho^+ \bar{\nu})$. Here, P_i and Ω_i ($i = \ell, \gamma, \rho$) are the momentum and solid angle, respectively, $m_{\pi\pi}$ is an invariant mass of $\pi\pi^0$ -system, and $\tilde{\Omega}_\pi$ is a solid angle of π in the $\pi\pi^0$ system. For the observable \vec{x} , we calculate the probability density function (PDF) $P(\vec{x})$ and the minimization of negative logarithmic likelihood function (NLL) allows one to get the best estimator of Michel parameters for a given set of \vec{x}_i ($i = 1, \dots, N$):

$$NLL = -\log L(\Theta) = -\sum_{i=1}^N \log P(\vec{x}_i), \quad (3.2)$$

where $\Theta = \{\eta, \rho, \xi, \xi \delta\}$ or $\Theta = \{\bar{\eta}, \xi \kappa\}$.

In our approach, the signal PDF is described analytically. As Fig. 4 shows, assuming the mass of neutrinos are zero, we can constrain the candidate of τ direction onto the arc. The visible PDF is then defined as integration of the initial differential cross section:

$$P^{\text{vis.}}(x) \equiv \frac{1}{\sigma_{\text{vis.}}} \frac{d\sigma_{\text{vis.}}}{d\vec{x}} = \frac{1}{\sigma} \int_{\Phi_1}^{\Phi_2} d\Phi \frac{d\sigma}{d\vec{x}d\Phi}. \quad (3.3)$$

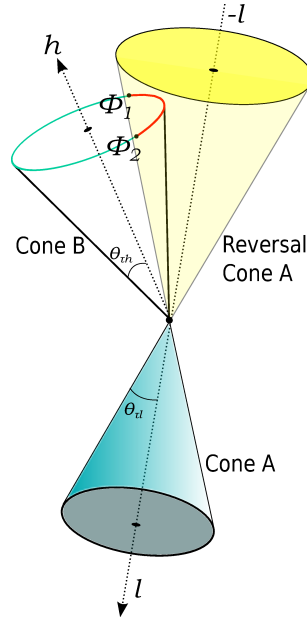


Figure 4: When one τ decays leptonically and the other τ decays hadronically, the direction of τ is constrained onto the arc in the center-of-mass system. The arc is an overlap of two cones that are defined around the direction of hadron and lepton momenta.

The differential cross section of $\tau^- \tau^+ \rightarrow (\ell^- \nu \bar{\nu})(\rho^+ \bar{\nu})$ decay is given as a linear combination in terms of Michel parameters: $d\sigma^{\text{vis.}}/d\vec{x} \propto \mathcal{C}_0(\vec{x}) + \mathcal{C}_1(\vec{x})\eta + \mathcal{C}_2(\vec{x})\rho + \mathcal{C}_3(\vec{x})\eta + \mathcal{C}_4(\vec{x})\xi + \mathcal{C}_5(\vec{x})\xi \delta$ for known functions $\mathcal{C}_i(\vec{x})$ ($i = 0, 1, \dots, 5$). Taking also into account the presence of event

Table 2: List of systematic uncertainty contributions

Item	$\sigma_{\bar{\eta}}^e$	$\sigma_{\xi\kappa}^e$	$\sigma_{\bar{\eta}}^\mu$	$\sigma_{\xi\kappa}^\mu$
Relative normalizations	4.2	0.94	0.15	0.04
Absolute normalizations	1.0	0.01	0.03	0.001
Description of the background PDF	2.5	0.24	0.67	0.22
Input of branching ratio	3.8	0.05	0.25	0.01
Effect of cluster merge in ECL	2.2	0.46	0.02	0.06
Detector resolution	0.74	0.20	0.22	0.02
Correction factor R	1.9	0.14	0.04	0.04
Beam energy spread	negligible	negligible	negligible	negligible
Total	7.0	1.1	0.76	0.24

selection efficiency, the normalized PDF is given by

$$\frac{1}{\sigma^{\text{vis.}}} \frac{d\sigma^{\text{vis.}}}{d\vec{x}} = \frac{[\mathcal{C}_0(\vec{x}) + \mathcal{C}_1(\vec{x})\eta + \mathcal{C}_2(\vec{x})\rho + \mathcal{C}_3(\vec{x})\eta + \mathcal{C}_4(\vec{x})\xi + \mathcal{C}_5(\vec{x})\xi\delta] \varepsilon(\vec{x})}{\int d\vec{x} [\mathcal{C}_0(\vec{x}) + \mathcal{C}_1(\vec{x})\eta + \mathcal{C}_2(\vec{x})\rho + \mathcal{C}_3(\vec{x})\eta + \mathcal{C}_4(\vec{x})\xi + \mathcal{C}_5(\vec{x})\xi\delta] \varepsilon(\vec{x})}, \quad (3.4)$$

where $\varepsilon(\vec{x})$ is a selection efficiency. The denominator of Eq. (3.4) is evaluated by Monte Carlo simulation and the difference of the factor of efficiency between the data and simulation $R(\vec{x}) \equiv \bar{\varepsilon}^{\text{data}}(\vec{x})/\bar{\varepsilon}^{\text{MC}}(\vec{x})$ is directly measured from real data.

We measure $R(\vec{x})$ values due to the corrections of ℓ^- identification, π^+ identification, π^0 reconstruction and trigger efficiency. Of all factors, the extraction of the trigger efficiency correction turns out to have the largest impact. In the current scheme, the expected systematic uncertainty is approximately 3% and we are investigating the procedure how to precisely measure the trigger efficiency correction. We aim to achieve the accuracy better than 1%, which is better than previous measurements.

3.4 $\bar{\eta}$ and $\xi\kappa$ measurement using $\tau^- \rightarrow \ell^- \nu \bar{\nu} \gamma$ decay

The measurement of $\bar{\eta}$ and $\xi\kappa$ using $\tau^- \rightarrow \ell^- \nu \bar{\nu} \gamma$ is carried out in the similar way as η, ρ, ξ and $\xi\delta$ analysis. Figure 5 shows the photon energy distribution for the muon decay mode $\tau^- \rightarrow \ell^- \nu \bar{\nu} \gamma$. Due to the background contamination to the signal photon candidates, the event selection suffers from the inclusion of backgrounds than $\tau^- \rightarrow \ell^- \nu \bar{\nu}$ case. The purity of signal events are approximately sixty percent for the muon mode.

In Table 2, we summarize the contributions of various sources of systematic uncertainties. The dominant systematic source for the electron mode is the calculation of the normalizations. Due to the peculiarity of the signal PDF when $m_l \rightarrow m_e$, the evaluation of the normalization factor is inaccurate and results in a notable effect. The uncertainty of the relative normalization is evaluated using the central limit theorem.

The largest systematic uncertainty for the muon mode is due to the limited precision of the description of background PDF. The set of minor background sources is treated as one additional

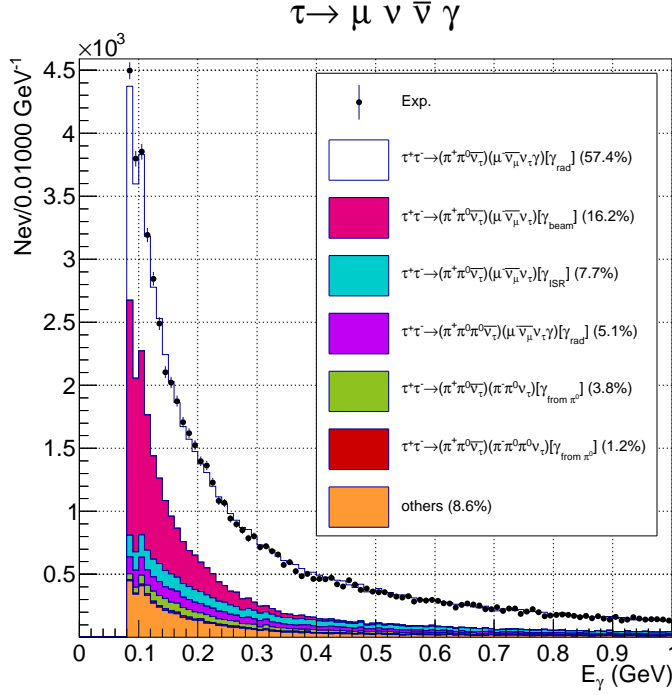


Figure 5: Distribution of the photon energy in the muon decay mode $\tau^- \rightarrow \mu^- \nu \bar{\nu} \gamma$. The empty and colored histograms are the signal and background Monte Carlo distributions. Dots with uncertainties are data.

category that is based on MC distributions. This effective description discards the information about correlations in the phase space and thereby gives significant bias.

Since the sensitivity to $\bar{\eta}$ is suppressed by the factor of m_l/m_τ , we extract it from the muon mode only. Using 832644 and 72768 selected events for $\tau^+\tau^- \rightarrow (\pi^+\pi^0\bar{\nu})(e^-\nu\bar{\nu}\gamma)$ and $\tau^+\tau^- \rightarrow (\pi^+\pi^0\bar{\nu})(\mu^-\nu\bar{\nu}\gamma)$ candidates, respectively, we obtain preliminary values

$$(\xi\kappa)^{(e)} = -0.5 \pm 0.8 \pm 1.1, \quad (3.5)$$

$$\bar{\eta}^\mu = -2.0 \pm 1.5 \pm 0.8, \quad (3.6)$$

$$(\xi\kappa)^{(\mu)} = 0.8 \pm 0.5 \pm 0.2, \quad (3.7)$$

where the first error is statistical and the second is systematic. The results of $\xi\kappa$ are combined to give

$$\xi\kappa = 0.6 \pm 0.4 \pm 0.2. \quad (3.8)$$

Figure 6 shows the contour the likelihood for $\tau \rightarrow \mu \nu \bar{\nu} \gamma$ events. As the shape suggests, a correlation between $\bar{\eta}$ and $\xi\kappa$ is small. The magnitude of the correlation coefficient determined by the error matrix is approximately 7%. This is the first experimental trial to measure the $\bar{\eta}$ and $\xi\kappa$ parameters.

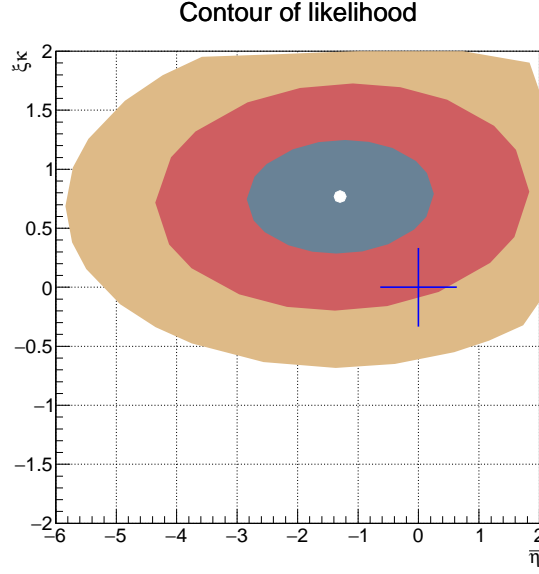


Figure 6: Contour of the likelihood for $\tau \rightarrow \mu \nu \bar{\nu} \gamma$ events. The circles indicate 1σ , 2σ and 3σ statistical deviations from inner to outer sides, respectively. The cross is the SM prediction.

4. Conclusion

Precision studies of leptonic decays of tau lepton is one of the most useful ways to search for the effects from New Physics. Of all strategies, measurement of Michel parameters allows us to verify the Lorentz structure of weak interaction in model independent way. Observing the ordinary leptonic decay, $\tau^- \rightarrow \ell^- \nu \bar{\nu}$, four Michel parameters η , ρ , ξ and $\xi\delta$ are measured whereas the radiative leptonic decay $\tau^- \rightarrow \ell^- \nu \bar{\nu} \gamma$ tells us information of spin of daughter lepton, which accordingly gives more two parameters $\bar{\eta}$ and $\xi\kappa$.

Using electron-positron colliders, various experiments had measured the four Michel parameters within a precision of a few percent. It is desired to update these measurement using modern B-factory apparatuses. On the other hand, the two parameters $\bar{\eta}$ and $\xi\kappa$ have not been measured.

Utilizing much abundant statistics of B-factory, Belle experiment tries to measure these six Michel parameters. In these measurements, it is important to extract the efficiency corrections precisely. Of all corrections, the factor of trigger efficiency turns out to have the largest systematic contribution. For η , ρ , ξ and $\xi\delta$ measurement, we are investigating the scheme to achieve precision better than 1%.

On the contrary, the uncertainty of $\bar{\eta}$ and $\xi\kappa$ measurements are dominated by statistical fluctuation. Based on 832644 and 72768 selected events for $\tau^+ \tau^- \rightarrow (\pi^+ \pi^0 \bar{\nu})(e^- \nu \bar{\nu} \gamma)$ and $\tau^+ \tau^- \rightarrow (\pi^+ \pi^0 \bar{\nu})(\mu^- \nu \bar{\nu} \gamma)$ candidates, respectively, we obtained preliminary result to be $(\xi\kappa)^{(e)} = -0.5 \pm 0.8 \pm 1.1$, $\bar{\eta}^{\mu} = -2.0 \pm 1.5 \pm 0.8$ and $(\xi\kappa)^{(\mu)} = 0.8 \pm 0.5 \pm 0.2$. These results are consistent with the SM prediction within their uncertainties. This is the first trial to measure $\bar{\eta}$ and $\xi\kappa$ parameters.

References

- [1] K.A. Olive *et al.* (Particle Data Group), *Chin. Phys.* **C38**, 090001 (2014).

- [2] L. Michel, Proc. Phys. Soc. A **63**, 514 (1950).
- [3] C. Bouchiat and L. Michel, Phys. Rev. **106**, 170 (1957).
- [4] W. Fetscher and H. J. Gerber, Adv. Ser. Direct. High Energy Phys. **14**, 657 (1995).
- [5] M. Fael, L. Mercolli and M. Passera, Phys. Rev. D **88**, no.9, 093011 (2013).
- [6] C. Fronsdal and H. Uberall, Phys. Rev. **113**, 654 (1939).
- [7] A. B. Arbuzov and T.V. Kopylova, JHEP. **1609**, 109 (2016).
- [8] Achim Stahl, Phys. Lett. B, **324**, 121 (1994).
- [9] Y. S. Tsai, Phys. Rev. D **4**, 2821 (1971).
- [10] W. Fetscher and H. J. Gerber, ETH-IMP PR-93-1 (1993).
- [11] A. Stahl and H. Voss, Z. Phys. **C74**, 73 (1997).
- [12] A. Heister *et al.* (ALEPH Collaboration), Eur. Phys. J. **C22**, 217 (2001).
- [13] J. P. Alexander *et al.* (CLEO Collaboration), Phys. Rev. D **56**, 5320 (1997).
- [14] A. Abashian *et al.*, Nucl. Instrum. Meth. A **479** 117 (2002)
- [15] A. Abdesselam *et al.* (Belle Collaboration), arXiv:1402.4969 (2014).
- [16] A. Abdesselam *et al.* (Belle Collaboration), arXiv:1609.08280 (2016).